Density distribution of a fluid through a microporous solid: Monte Carlo simulation

W. Dong and B. Bigot
Groupe de Chimie Théorique, Institut de Recherche sur la Catalyse, Centre National de la Recherche Scientifique, 2, Avenue Albert Einstein, 69626 Villeurbanne Cedex, France
and Ecole Normale Supérieure de Lyon, 46, Allée d'Italie, 69364 Lyon Cedex 07, France
(Received 5 August 1993)

A simple model is proposed for an inhomogeneous system consisting of a fluid and a microporous solid. In the proposed model, the interfacial region near the outer surface of the porous solid is described explicitly. Monte Carlo simulations are carried out to determine the fluid density distribution through the microporous solid. It is found that the lateral density variation is as important as that in the direction perpendicular to the outer solid surface. A theoretical approach based on the Kirkwood superposition approximation is proposed and tested against the simulation results. Such an approach gives a satisfactory qualitative (even quantitative in some cases) description of the density distribution in the model system.

PACS number(s): 68.45.−v, 61.20.Ja

I. INTRODUCTION

In the last years, the study of fluids confined in microporous media has attracted much attention. This is motivated by the wide applications involving microporous media, e.g., heterogeneous catalysis by zeolites, petroleum recovery from porous rocks, and membrane separation processes. A variety of structural, thermodynamic and transport properties of some model porous systems have been studied by simulations and theoretical approaches. The narrow slit pore is the most studied model. The pore walls are modeled either by smooth surfaces [1–4] or by structured surfaces with discrete interaction sites [5–8]. The smooth and structured wall models for a cylindrical pore were also studied by various simulation methods [9–11]. In a microporous medium, the broken translational symmetry in certain directions induces inhomogeneity in the density distribution of a fluid confined in it. Therefore, the determination of the spatial distribution of fluid molecules has obvious importance in understanding, at a molecular level, the thermodynamic and transport properties of fluids confined in or going through a porous medium. Previous works (all those cited above) have exclusively focused on the fluid structures and thermodynamic properties in the deep interior region of a microporous sample. In a grand-canonical-ensemble Monte Carlo (MC) simulation [2], such a deep interior region is related to the outside bulk fluid through a constant chemical potential and the bulk fluid is not explicitly described at all. When a Gibbs ensemble Monte Carlo simulation [11] is carried out, the outside bulk fluid phase and the deep interior fluid-pore phase are investigated simultaneously. As its characteristic feature, the interfacial region between the bulk fluid phase and the outer surface of the porous solid is not described explicitly. Structures and phenomena in this interfacial region were not studied until the recent work of Yethiraj and Hall [12]. Nevertheless, this exterior interfacial region can play an important role in some processes. We would like to mention the dynamic process of molecules entering pores. Under some conditions this process can become the limiting step. If the microporous medium under consideration is a zeolite, its catalytic property can thus be affected. It is well known that an impermeable solid surface induces inhomogeneity in the vicinity of solid-fluid interface. One expects that near the permeable surface of a microporous solid, nonuniform distribution of fluid arises also. Moreover, there will be inhomogeneity not only in the direction perpendicular to the interface but also in the parallel directions. Before carrying out an investigation of the transport properties through a porous medium, it is desirable to have first some detailed structural information. They will supply us valuable insight based on the potential of mean force exerted on a fluid particle. In this work, we present a simulation study of a simple model for a fluid through a microporous solid. The model and the simulation method are described in the next section. In Sec. III, simulation results are presented and it is also shown that a simple theoretical approach based on the Kirkwood superposition approximation reproduces well the qualitative feature of the simulation results for the density distribution. Concluding remarks are given in the last section.

II. MODEL AND SIMULATION METHOD

A. Model

The outer surface of a microporous sample is, in general, a structured one due to the presence of pore entries. In contrast to a smooth surface, the fluid density distribution function varies not only in the direction perpendicular to but also parallel to a structured surface. A complete determination of the one-body distribution function necessitates, in this case, space resolution in directions parallel to the interface. To our knowledge, no such complete determination of the density distribution function has been reported for any structured surface. The

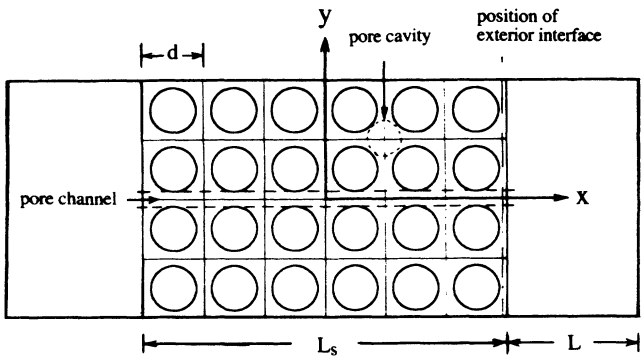

FIG. 1. Simulation box geometry and definition of coordinate system.

obvious reason is that such a type of investigation needs too much computation in order to obtain reasonable statistical accuracy. A common practice [5–8] is to determine only the variation perpendicular to the interface and take average in the parallel directions. Very recently, Vermesse and Levesque have also studied partially averaged density profiles near a microporous surface [13]. In the present work, we proceed to make a complete determination of the one-body distribution function of a fluid through a microporous solid. Since space resolutions in both parallel and perpendicular directions necessitate considerable computational resources, we restrict ourselves to a two-dimensional model. To a first approximation, a porous medium can be described simply by a model in which a portion of space is inaccessible to fluid molecules and the rest of the space forms the pores in which the fluid molecules can move. In this work, the microporous solid is modeled by a regular lattice which contains an ensemble of hard disks fixed on it. A schematic presentation is given in Fig. 1. The space occupied by these fixed disks is inaccessible to fluid particles. The interstitial space represents the pores. From Fig. 1 it is clear that there is a network of pore cavities that are connected to each other by four bottleneck passages. This geometrical aspect has some resemblance to certain A-type zeolites [14]. For a simple description of fluid molecules, we choose the hard-disk model. Although the above model for a fluid-porous solid system is a very idealized one, we expect it can supply some qualitative insight into the structure of such systems. In the next section, it will be shown that this simple model can indeed create quite rich variations of density distribution.

B. Simulation method

To study the model described above, Monte Carlo simulations are carried out. The central simulation box (a two-dimensional one) is constructed as follows. A slab of porous solid is placed in the middle of the box (see Fig. 1). The thickness of this slab, L_s, should be large enough to avoid the influence of one outer surface of the porous solid upon the other one. The conventional periodic conditions are applied in both x and y directions (see Fig. 1 for the definition of the coordinate system). The length of the outer space, L, which contains only the fluid phase, must be large enough to avoid any interactions between outer surfaces and their images. The canonical ensemble Monte Carlo simulation is performed for the entire system. Such a supercomposite system contains two subsystems, i.e., the microporous solid with adsorbed fluid particles in it and the bulk fluid phase outside it. These two subsystems are in thermodynamic equilibrium. They can of course exchange particles. The interfacial structures and phenomena taking place near the outer surface of a porous solid can only be studied in such a way that the two subsystems are brought in physical contact. The above simulation procedure is in the same spirit as that used by Yethiraj and Hall for their study of a fluid through a single slit pore [12].

For a practical implementation to simulate the above model, one can make a straightforward adaptation of a standard method for a binary mixture. The only modification to be introduced consists of keeping the particles of one component fixed on a lattice during the whole simulation. Thus, all the particles of this component with a frozen configuration constitute the microporous solid of our model. When using this method, the amount of computations for the interactions between fluid particles and the frozen solid particles (or the calculations of the corresponding interparticle distances) is proportional to NN_s, with N and N_s being, respectively, the number of fluid particles and that of solid particles. In fact, a more efficient method can be devised which reduces the above calculations to an amount proportional to N. First, the space occupied by the porous solid is divided into small cells in such a way that each cell contains one frozen solid particle which is placed at the center of the corresponding cell (see Fig. 1). It is obvious that the side length of such a cell (denoted by d in Fig. 1) is equal to the distance between two nearest solid particles. Only when a fluid particle enters into the porous solid, is there the need to test whether overlapping with a solid particle occurs. This can be done in the following way:

$$r>(\sigma+\sigma_s)/2\ ,\quad \text{nonoverlapping}\ ,$$

$$r<(\sigma+\sigma_s)/2\ ,\quad \text{overlapping}\ ,$$

$$r=[(x-c_x)^2+(y-c_y)^2]^{1/2}\ ,$$

where σ and σ_s are, respectively, fluid- and solid-particle diameters, (x,y) is the position of the fluid particle under consideration, and (c_x,c_y) is the position of the solid particle which is nearest to the fluid particle under consideration. Knowing (x,y), one can determine quite easily (c_x,c_y). The computational advantage of this method is that to test the overlapping of a fluid particle with a solid particle, one needs only to calculate the distance between the fluid particle and the solid particle nearest to it but not any other solid particles. It is this method that we use to obtain the results to be presented in the next section.

III. RESULTS AND DISCUSSIONS

The microporous solid model described in the last section is completely defined by the solid-particle diameter, σ_s, the size of the unit cell d, and the manner in which the solid lattice is cut to make its outer surface. In the notation of crystallography, the outer surface of the model depicted in Fig. 1 can be denoted as a (1,0) surface. It is noteworthy that for our two-dimensional model the surface reduces just to a line. The size of the porous solid sample can be given by specifying the number of unit cells in the x and y directions, n_{cx}, n_{cy}. The computational conditions are fully specified when the fluid particle diameter σ, the number of fluid particles in the simulation box N, and the length of the outer space L (see Fig. 1) are given together with the above parameters defining the porous solid. We have carried out simulations with several sets of the above parameters. In Table I the computational conditions are summarized. The fluid-particle diameter is chosen as our length unit.

From the parameters given in Table I, one can calculate the nominal total fluid density ρ_T, which is also listed in Table I. The systems we have studied correspond to typical liquid densities. The actual density of the bulk fluid phase outside the porous solid and that inside it can be found only after simulation results are obtained. In Table I we also give the number of configurations N_{cf}, from which statistical calculations are made. The principal structural quantity we are interested in is the one-body distribution function $\rho(\mathbf{r})$. It is determined from a histogram of fluid-particle configurations, i.e.,

$$\rho(\mathbf{r})=\rho(x,y)=\langle N(x,x+\Delta x;y,y+\Delta y)\rangle/\Delta x\,\Delta y\ , \qquad (1)$$

where $\langle N(x,x+\Delta x;y,y+\Delta y)\rangle$ is the mean fluid particle number within a small element $\Delta x\,\Delta y$ near a point (x,y). The space resolution is

$$\Delta x=\Delta y=0.05\sigma$$

TABLE I. Computational parameters.

No.	Surface	σ_s/σ	d/σ	n_{cx}	n_{cy}	N	L/σ	$\rho_T\sigma^2$	$10^{-5}N_{cf}$
I	(1,0)	2.0	4.0	6	4	336	8.0	0.5951	3.6
II	(1,0)	6.0	8.0	4	4	645	8.0	0.5952	3.05
III	(1,0)	5.0	8.0	4	4	670	6.0	0.6125	2.98
IV	(1,1)	2.0	$4\sqrt{2}$	4	4	527	$6\sqrt{2}$	0.5996	3.0

in the case of a (1,0) surface, and $(\sqrt{2}/28)\sigma$ for a (1,1) surface.

One main computational difficulty for determining the one-body distribution function resolved in all directions (both x and y in our case) is that for sufficiently fine space resolutions one needs quite large statistical samples. Therefore, any statistical error reducing procedure is highly desirable. To improve the statistical accuracy for the systems considered in this work, one can take advantage of the periodicity in the direction parallel to the outer surface of the solid and the reflection symmetries about the x and y axes. For all the results to be presented below, we average the values of $\rho(\mathbf{r})$ in all the regions that are symmetrically equivalent. Before applying the above procedure to improve statistical accuracy, we note each time that the periodicity and symmetries are well respected by $\rho(\mathbf{r})$ obtained directly from the raw simulation results.

In Fig. 2 we plot the part of the one-body distribution function outside the microporous solid. The common feature one observes here is that the fluid has a multilayer structure near the outer surface of the microporous solid. The first layer consists of peaks with a large amplitude. They are situated in front of the solid particles of the outer surface. In front of pore openings, one finds secondary maxima. The number of such secondary maxima increases when the pore opening becomes larger. In the

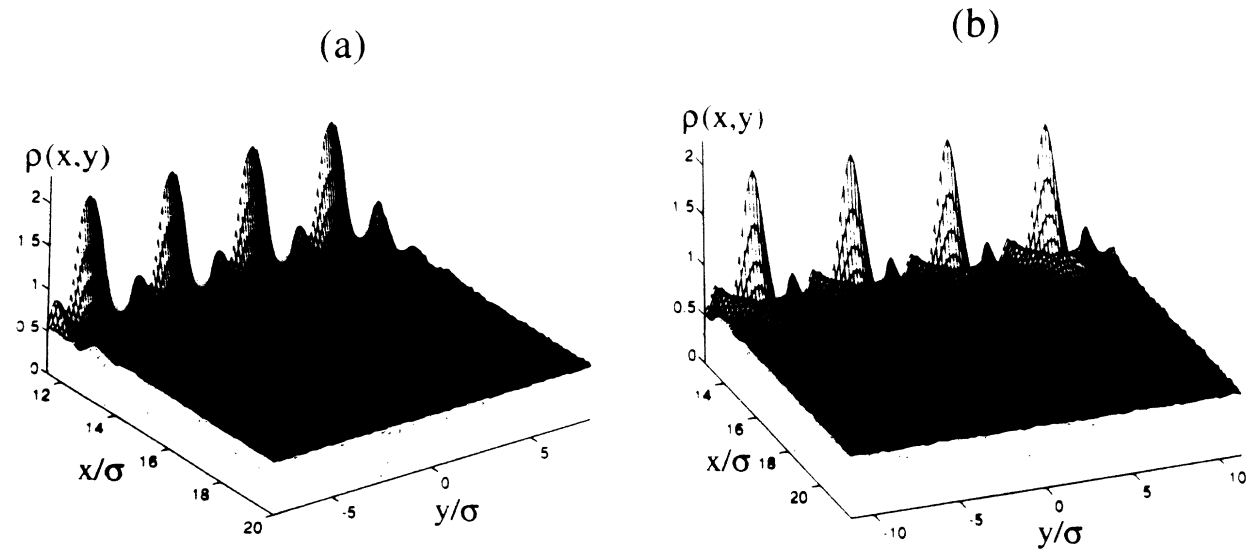

FIG. 2. Density distribution function (plotted from outer surface to bulk fluid phase). (a) $d=4\sigma$, $\sigma_s=2\sigma$, and (1,0) surface; (b) $d=4\sigma$, $\sigma_s=2\sigma$, and (1,1) surface.

case of a (1,0) surface with $d=4\sigma$, there is only one which results from a kind of constructive interference of the second fluid layer around each solid particle [see Fig. 2(a)]. In the other cases with larger pore openings, the second fluid layers around two nearby solid particles do not overlap. Hence, two secondary maxima are found in front of each pore opening. Figure 2(b) gives an illustration that corresponds to case IV in Table I. Under the other conditions given in Table I, quite similar results are obtained. From these results, one may note already that in the regions where a fluid particle is not strongly affected by the simultaneous presence of several solid particles, the fluid structure is similar to that around a single immobile solid particle. One can see this more clearly in Fig. 3, in which we give a presentation that reveals the general features of $\rho(\mathbf{r})$ in the whole system, i.e., inside as well as outside the porous solid.

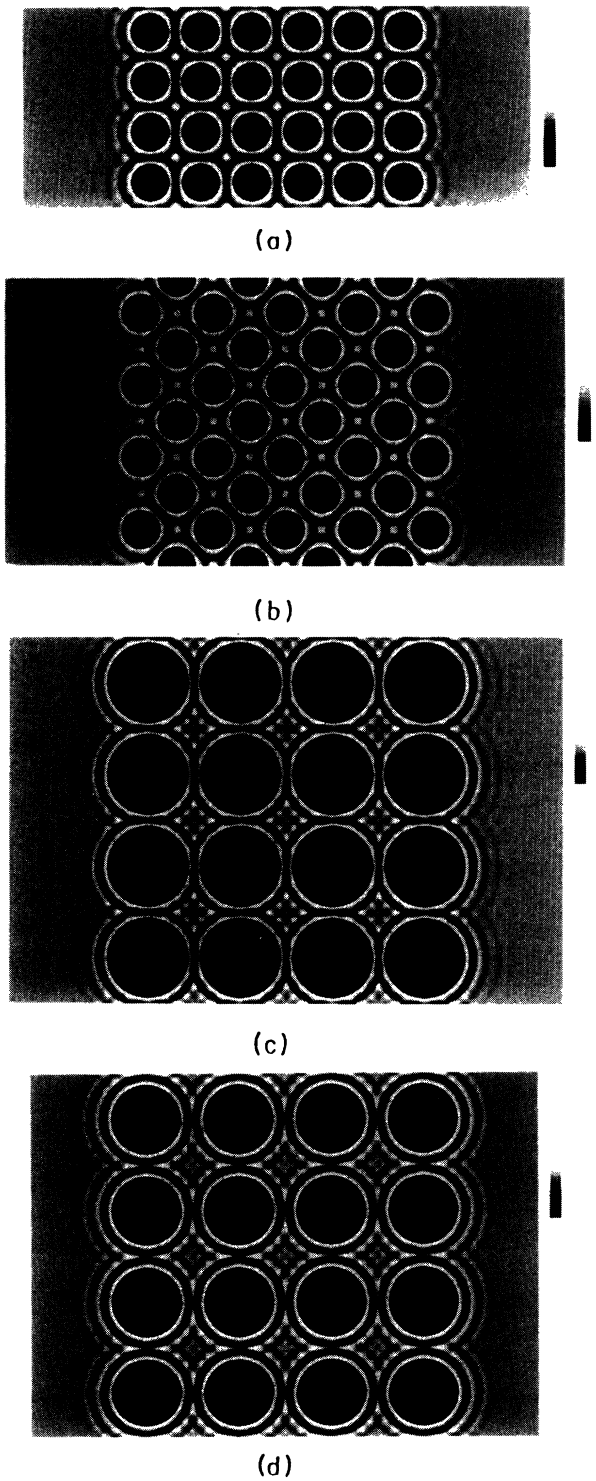

FIG. 3. Two-dimensional projection of density distribution function. (a) $d=4\sigma$, $\sigma_s=2\sigma$, and (1,0) surface; (b) $d=4\sigma$, $\sigma_s=2\sigma$, and (1,1) surface; (c) $d=8\sigma$, $\sigma_s=6\sigma$, and (1,0) surface; (d) $d=8\sigma$, $\sigma_s=5\sigma$, and (1,0) surface.

In Fig. 3, the one-body distribution function is projected onto a plane. The variation of the function is expressed by the variation of the brightness of these images and a brighter region has larger values of $\rho(\mathbf{r})$. The darkest regions are those occupied by solid particles where the probability of finding a fluid particle is strictly zero. In Figs. 3(a) and 3(b), the results for $d=4\sigma$ and $\sigma_s=2\sigma$ are given. The only difference between them is that Fig. 3(a) presents the result for a (1,0) surface while Fig 3(b) presents the result for a (1,1) surface. As one can expect, in the interior of the porous solid the fluid particles are distributed in the same way in the two cases except that the solid lattices are orientated differently. Around each solid particle, there is one layer of adsorbed fluid particles which is not much perturbed by the presence of other solid particles nearby. The local number density in this layer is much higher than that of the bulk fluid outside the porous solid. In the pore cavities away from the pore walls, the density is, in general, low. At the center of each pore cavity there is also a local maximum of $\rho(\mathbf{r})$ but the amplitude is much smaller than the contact value near a solid particle. When the size of the unit cell is increased, the pore cavity also becomes larger. Then new local maxima appear in the pore cavities [see Figs. 3(c) and 3(d)]. For all the cases shown in Fig. 3 it is seen that the first layer of adsorbed fluid around a solid particle is not much affected by the presence of the other solid particles and there is a striking reminiscence of the structure of a fluid around a single immobile solid particle. This has motivated us to examine whether a theoretical approach based on the superposition approximation can reproduce the fluid structure observed here. For the model system considered in this work, the one-body distribution function of the inhomogeneous system can be equivalently regarded as the conditional probability to find a fluid particle knowing that a set of solid particles are fixed on a lattice. Therefore, a superposition approximation à la Kirkwood can be written as

$$\rho^{\mathrm{sa}}(\mathbf{r})=\rho_{b1}\prod_{i=1}^{N_s} g(|\mathbf{r}-\mathbf{R}_i|)\ , \tag{2}$$

where ρ_{b1} is the density of the bulk fluid phase outside the porous solid, and $g(|\mathbf{r}-\mathbf{R}_i|)$ is the fluid radial distribution function around a solid particle located at $\mathbf{R}_i$. Obviously $\mathbf{R}_i$'s are lattice vectors of the porous solid. The legitimate validity of the superposition approximation is in the asymptotic region where the solid particles are distant from each other. Often it is not clear to what extent the superposition approximation holds. In the fol-

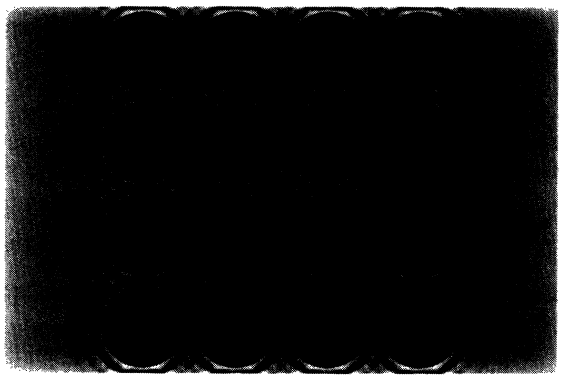

FIG. 4. Two-dimensional projection of $\rho^{sa}(x,y)$. $d=8\sigma$, $\sigma_s=6\sigma$, and (1,0) surface.

lowing, we will show that for the model considered here, the superposition approximation performs quite well even in the cases that cannot be considered *a priori* as being in the asymptotic region.

In order to determine $\rho^{sa}(\mathbf{r})$, one has to supply the radial distribution function in Eq. (2). The radial distribution functions we used to calculate $\rho^{sa}(\mathbf{r})$ are the exact ones determined also from MC simulations. In this way one avoids additional approximations related to the determination of radial distribution functions. Thus, any inaccuracy that one finds is that inherent to the superposition approximation. In order to make a comparison between $\rho^{sa}(\mathbf{r})$ and the exact result of $\rho(\mathbf{r})$, MC simulations are also carried out for a hard-disk fluid around a single immobile hard disk with diameters of 2σ, 5σ, and 6σ. We find that the superposition approximation gives very satisfactory qualitative results. In Fig. 4, a projected image of the one-body distribution function given by the superposition approximation is shown for the cases of $d=8\sigma$ and $\sigma_s=6\sigma$. This image is nearly indistinguishable from that given in Fig. 3(c). It is remarkable that the superposition approximation reproduces exactly the same pattern of the density variation, i.e., the same number of local maxima in each pore cavity and at the same positions as that found from simulations. However, this projected presentation does not allow precise comparison of amplitudes. More detailed quantitative comparison can be made by scrutinizing various density profiles.

First we will examine the lateral density variation near the outer surface, i.e., in the parallel direction. For this purpose, we plot density profiles as a function of y with x fixed to a specified value. In Fig. 5, density profiles at several distances from the outer surface ($\delta x=0.0$, 0.5σ, 1.2σ, and 2.0σ) are presented. Here, only the results corresponding to case I in Table I are shown. These results complement those presented in Fig. 2(a) by displaying more details about the lateral density distribution. For all the cases, the dot-line curve (superposition approximation result) overlaps perfectly the full-line curve (simulation result). The superposition approximation reproduces extremely well the simulation results for the lateral density variations outside the exterior surface. This is

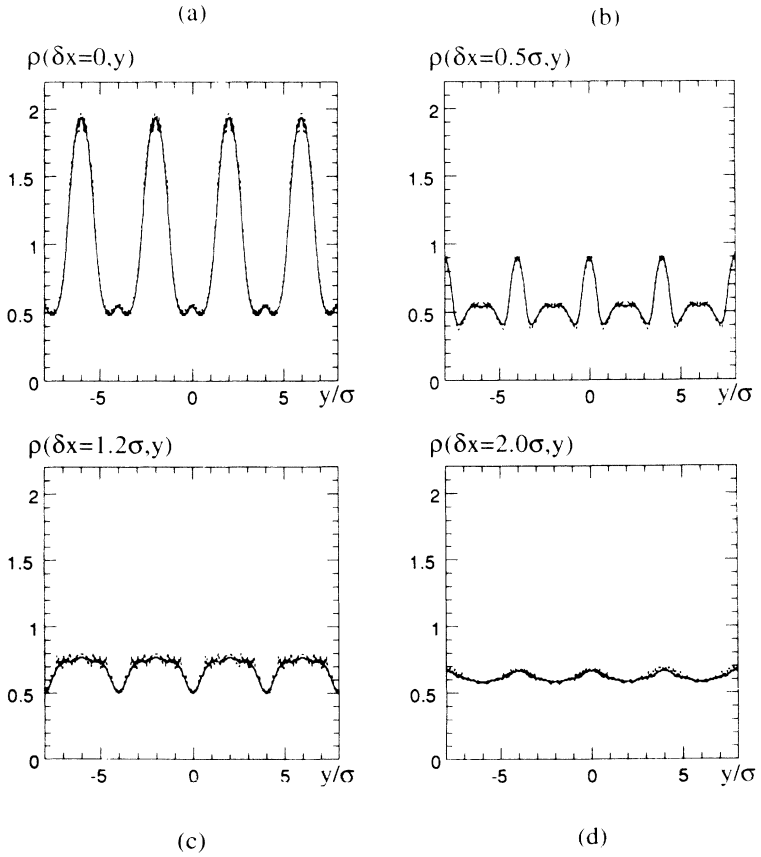

FIG. 5. Density profiles for lateral variation $d=4\sigma$, $\sigma_s=2\sigma$, and (1,0) surface. ——, MC simulation; — — —, superposition approximation.

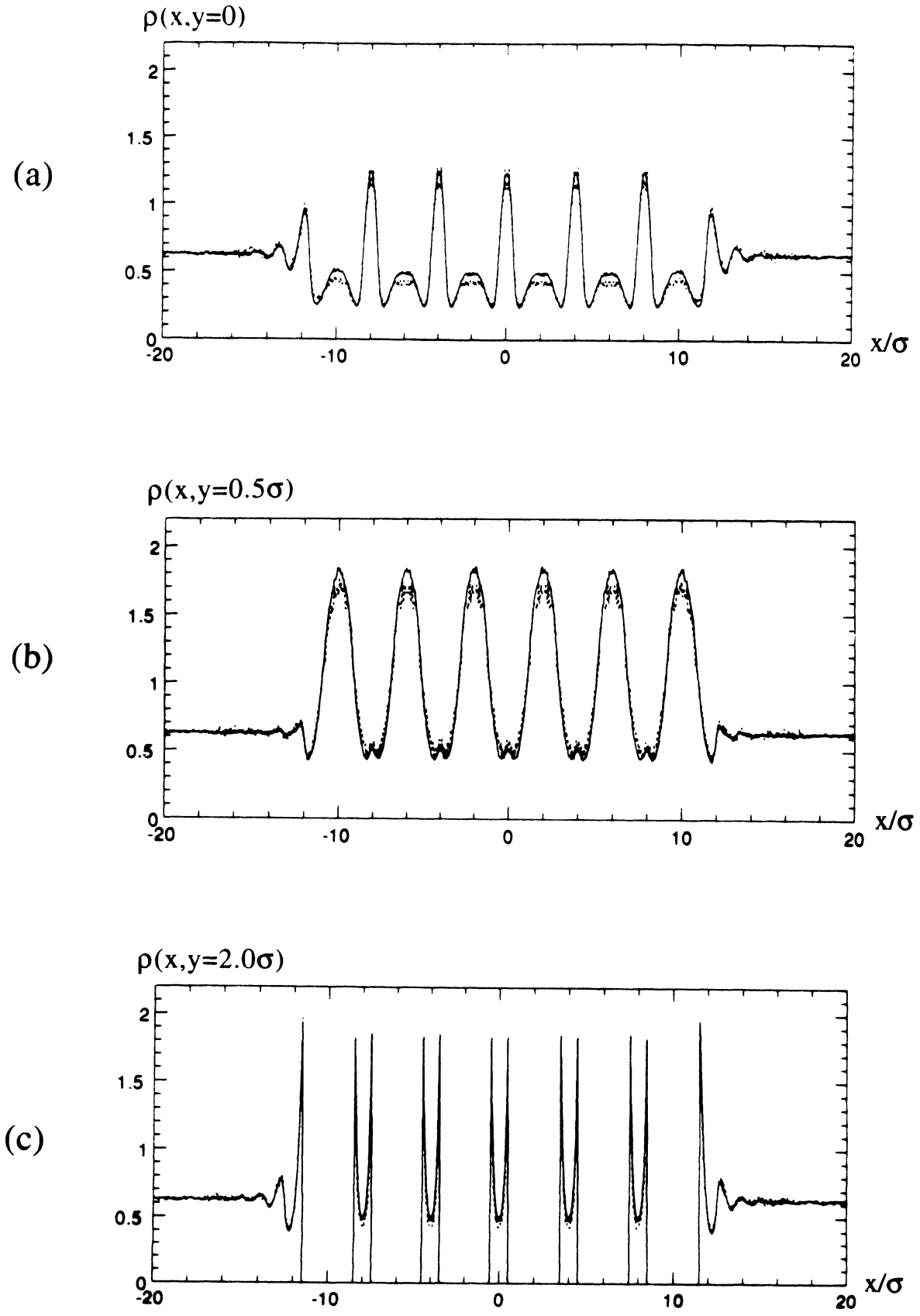

FIG. 6. Density profiles for variation perpendicular to outer solid surface. $d=4\sigma$, $\sigma_s=2\sigma$, and (1,0) surface. —— MC simulation; — — —, superposition approximation.

also true under the other conditions given in Table I.

To get a conclusive appraisal of the superposition approximation, it is necessary to see also how well it can describe the density variations inside the porous solid. For this purpose one can examine the density variations through the porous solid sample, i.e., in the direction perpendicular to the outer surface. Now the density profiles to be considered are a function of x with y having fixed value. Taking into account the symmetry of the system, one needs only to consider the fixed values of y in the region from $y=0$ to $y=d/2$ since any other value of y is a symmetrically equivalent one of this region due to the periodicity of the system in the y direction.

In Fig. 6 we show three density profiles through the porous solid for the case of $d=4\sigma$ and $\sigma_s=2\sigma$ with a (1,0) surface. The first density profile [see Fig. 6(a)] describes the density variation along the axis of a straight pore channel going through the whole porous sample. The fixed value of y for the second profile ($y=0.5\sigma$) defines the boundary of the above pore channel since the fluid particles begin to touch solid particles but no inaccessible regions are crossed yet. For these two density profiles [Figs. 6(a) and 6(b)], the superposition approximation underestimates the fluid density in the zones of the narrow passages connecting pore cavities. In the region of $y=0.5\sigma$ to $y=d/2$, some portions of the density profile drop to zero in the inaccessible zones occupied by solid particles. In the whole region of $y=0.5\sigma$ to $y=d/2$, there are two peaks in the interstitial zone between two solid particles. Here we show just the profile at $y=d/2$ [see Fig. 6(c)]. From Fig. 6(c), it appears that for this value of y the superposition approximation gives a nearly perfect fit of the exact simulation results. This is indeed the case near the outer surface. But inside the porous solid, the peaks of the dot line given by the superposition approximation are in fact lower than the exact ones by 7%. This is not evidenced in the figure because of line overlappings.

From the above results, one observes that in the regions corresponding to the pore cavities, the superposition approximation works very well. A discrepancy is found in the regions where fluid particles are more confined by the presence of solid particles, i.e., near the bottleneck passage connecting two pore cavities. This is a general feature which holds also under the other conditions given in Table I. It is not difficult to understand this. In these more confining regions, the correlation of a fluid particle with two solid particles nearby becomes stronger and this three-body correlation effect is not taken into account in the superposition approximation given in Eq. (2). This is the reason why the superposition approximation is less accurate in a more confining region. This enables one also to understand why more accurate results can be obtained from the superposition approximation when the connecting passage size is increased. Although not shown here, it should be mentioned that in the case of $d=8\sigma$ and $\sigma_s=5\sigma$ the superposition approximation gives quantitatively accurate results. In spite of discrepancies in some regions for the other cases, we find that the superposition approximation gives quite satisfactory qualitative results especially in view of its simplicity.

Finally, in Fig. 7, we present the density profile obtained by averaging the one-body distribution function in the direction parallel to the outer surface, i.e.,

$$\rho_{\mathrm{av}}(x)=\langle N(x,x+\Delta x)\rangle/\Delta V_{\mathrm{void}}\ , \tag{3}$$

where $\langle N(x,x+\Delta x)\rangle$ is the mean number of fluid particles falling in a slice between x and $x+\Delta x$ and ΔV_{void} is the void volume in the slice. The mean density profiles presented in Fig. 7 is quite different from those given in Fig. 6. This shows clearly that what happens locally can be quite different from what one might imagine from a mean density profile. Therefore, the mean density profile has a limited ability to supply structural information of highly inhomogeneous systems with inhomogeneity in all the directions.

The macroscopic quantity which can give a global idea about the fluid partition is the partition coefficient defined as

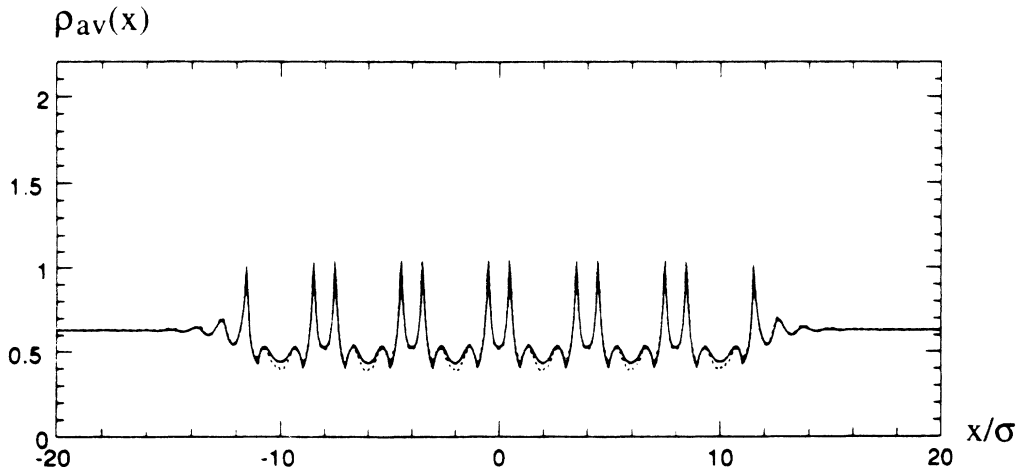

FIG. 7. Mean density profiles. —— MC simulation; — — —, superposition approximation. $d=4\sigma$, $\sigma_s=2\sigma$, and (1,0) surface.

TABLE II. Partition coefficient and bulk fluid densities inside and outside porous solid.

No.	α	ρ_{1b}	ρ_{2b}
I	0.9051	0.6279	0.5683
II	0.9034	0.6271	0.5665
III	0.9361	0.6389	0.5981

$$\alpha=\rho_{b2}/\rho_{b1} , \tag{4}$$

where ρ_{b1} has been defined before [see Eq. (2)] and ρ_{b2} is the mean fluid density in the interior of the microporous solid. The results for the partition coefficient are given in Table II together with the values of ρ_{b1} and ρ_{b2}. When ρ_{b2} is calculated, only the unit cells in the deep interior of the porous solid are taken into account to avoid surface effect near the outer fluid-solid interface. Under all the conditions considered here, we have found that $\alpha<1$. In the absence of attractive forces between fluid particles and the porous solid, the porous medium is depleted of fluid by about 10% for the cases examined in this work.

IV. CONCLUSIONS

In the present work, MC simulations are carried out for a simple model of a fluid through a microporous solid. Our canonical ensemble Monte Carlo simulation is performed on a supersystem which contains both the fluid confined in the porous solid and the bulk fluid phase outside it. In this way, one can study the fluid structure near the outer surface of a microporous solid. In this interfacial region, one observes a multilayer structure as in the case of an impermeable solid surface. The periodic array of the surface solid particles and the pore openings induces also large lateral density variations near the outer porous solid surface. Inside the microporous solid, the fluid-particle distribution is perfectly modulated by the periodicity of the solid lattice. The local density near the pore walls is higher than that in the pore cavities.

One goal of the present work is to gain some insights which are helpful for developing theoretical approaches. The fact that the fluid structure around each solid particle is strongly reminiscent of that around a single isolated solid particle has motivated us to propose an approach based on the Kirkwood superposition approximation. Comparison with simulation results shows that this approach gives a satisfactory qualitative description of the density distribution of our model fluid–porous-solid system. When the sizes of the narrowest places in the porous solid is more than three times the diameter of a fluid molecule, the superposition approximation becomes quantitatively accurate.

For a highly inhomogeneous system, i.e., with inhomogeneity in all directions, precise information about the density distribution can be only obtained from the complete distribution function. It is shown that the mean density profile, i.e., averaged in certain directions, has limited application for understanding the fluid distribution. What happens locally can be very different from what one may imagine from the averaged profile. We believe that this point is a quite general one for highly inhomogeneous systems although it is evidenced by the very simple model studied here.

ACKNOWLEDGMENTS

The authors thank Dr. F. Vigné-Maeder and Dr. M. Kolb for many interesting discussions.

[1] W. van Megen and I. K. Snook, J. Chem. Soc. Faraday Trans. 2 **75**, 1095 (1979).
[2] I. K. Snook and W. van Megen, J. Chem. Phys. **72**, 2907 (1980).
[3] W. van Megen and I. K. Snook, Mol. Phys. **54**, 741 (1985).
[4] J. J. Magda, M. Tirrel, and H. T. Davis, J. Chem. Phys. **83**, 1888 (1985).
[5] S. Toxaerd, J. Chem. Phys. **74**, 1998 (1981).
[6] M. Schoen, D. J. Diestler, and J. H. Cushman, J. Chem. Phys. **87**, 5464 (1987).
[7] M. Schoen, J. H. Cushman, D. J. Diestler, and C. L. Rhykerd, J. Chem. Phys. **88**, 1394 (1988).
[8] J. H. Sikkenk, J. O. Indenkeu, J. M. J. van Leeuwen, and E. O. Vossnack, Phys. Rev. Lett. **59**, 98 (1987).
[9] G. S. Heffelfinger, F. van Swol, and K. E. Gubbins, Mol. Phys. **61**, 1381 (1987).
[10] B. K. Peterson and K. E. Gubbins, Mol. Phys. **62**, 215 (1987).
[11] A. Z. Panagiotopoulos, Mol. Phys. **62**, 701 (1987).
[12] A. Yethiraj and C. K. Hall, Mol. Phys. **73**, 503 (1991).
[13] J. Vermesse and D. Levesque, Mol. Phys. **77**, 837 (1992).
[14] J. M. Shin, K. T. No, and M. S. Jhon, J. Phys. Chem. **92**, 4533 (1988).

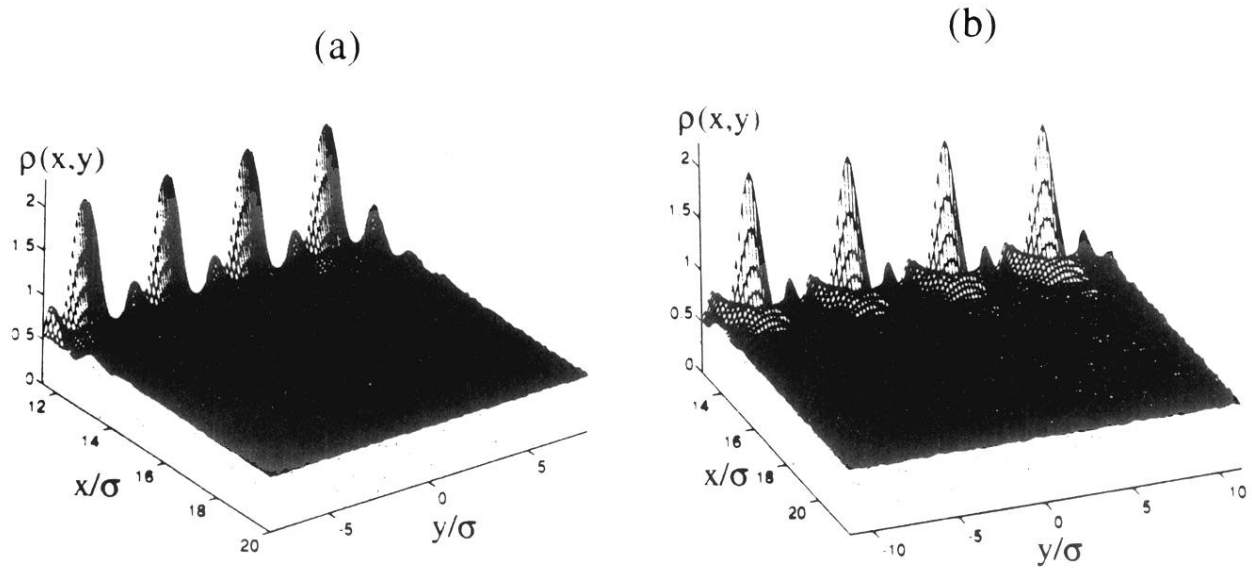

FIG. 2. Density distribution function (plotted from outer surface to bulk fluid phase). (a) $d=4\sigma$, $\sigma_s=2\sigma$, and (1,0) surface; (b) $d=4\sigma$, $\sigma_s=2\sigma$, and (1,1) surface.

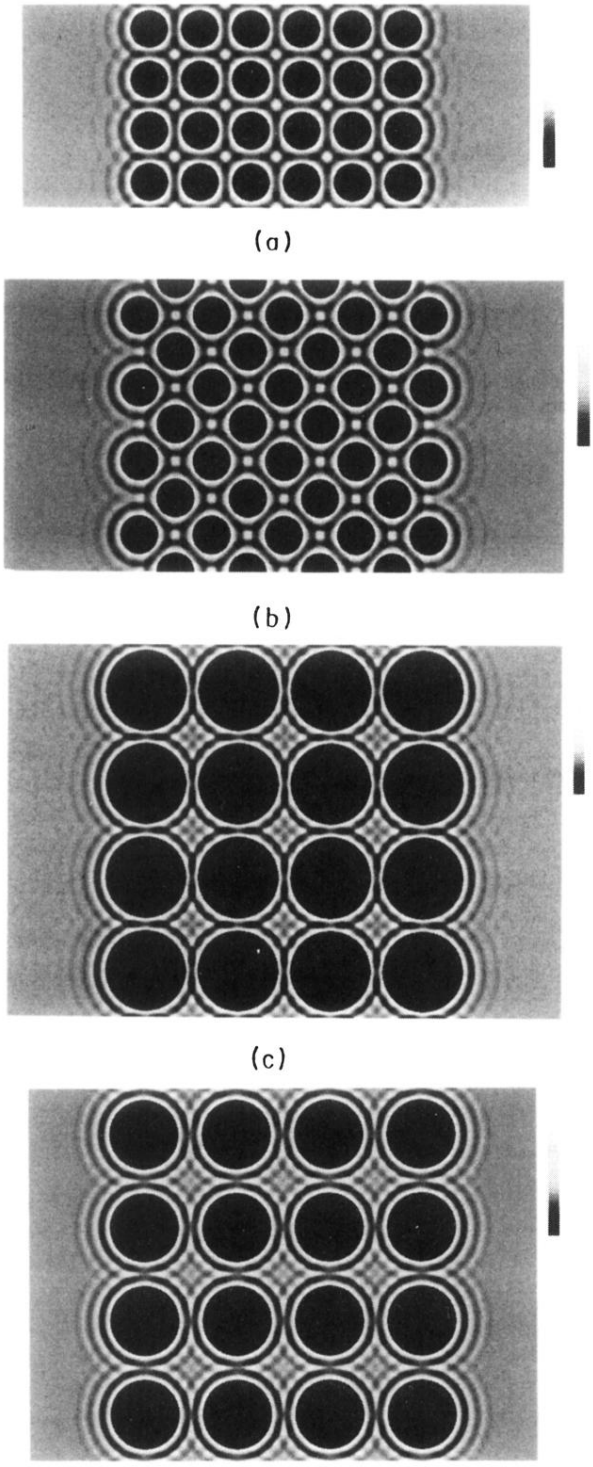

FIG. 3. Two-dimensional projection of density distribution function. (a) $d=4\sigma$, $\sigma_s=2\sigma$, and (1,0) surface; (b) $d=4\sigma$, $\sigma_s=2\sigma$, and (1,1) surface; (c) $d=8\sigma$, $\sigma_s=6\sigma$, and (1,0) surface; (d) $d=8\sigma$, $\sigma_s=5\sigma$, and (1,0) surface.

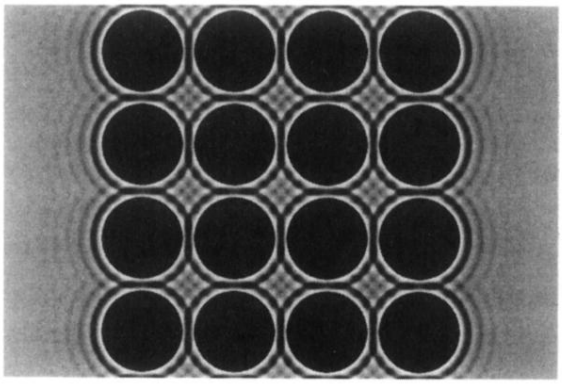

FIG. 4. Two-dimensional projection of $\rho^{sa}(x,y)$. $d=8\sigma$, $\sigma_s=6\sigma$, and (1,0) surface.